Flight Stabilization of Micro Motor Flapping Wing Micro Aerial Vehicle

Vikash Balasubramanian, Andrew Fassler, and Ramon Rijos
24-675, Micro/Nano-Robotics, Spring 2013
Final Project Mid-Semester Report

Abstract:

The forces acting on flapping wing micro aerial vehicle are briefly analyzed to determine why these robots are unstable. A passive stabilization system for a flapping wing micro aerial vehicle composed of a tail fin is proposed and tested, the results of which are compared to vehicle without the stabilization system. Results show that the tail fin increases flight time before destabilization, but the total flight time is still very limited. Additional tests are also performed to determine the lift and thrust forces generated by a wing flapping.

Introduction:

Research on Flapping Wing Micro Aerial Vehicles (FWMAV) stems from the attempt to create micro scale flying robots inspired by dipteran insects, such as the fruit fly. This field has seen many breakthroughs in recent years, including the creation of devices able to achieve liftoff and autonomous flight [1-7]. Still, many FWMAV's must operate with tethers and on guide rails as they often have difficulty in maintaining stability once they achieve flight, lacking any passive or active balance control [5]. Inclusion of such a device would enable FWMAV's to maintain a hover to allow for sustained flight. Without any form of stabilization, any asymmetry of the forces acting on the FWMAV will cause it to tilt and rotate while flying, further destabilizing it and leading it to crash. We propose to create a passive stabilization device to help balance the forces acting on a FWMAV such that it can lift off and maintain flight.

The system we are using for our FWMAV utilizes two micro rotary motors to achieve flight, each one directing power to an individual wing as demonstrated by Hines et al [8]. The rotary motors are powered by an AC power supply to create the cyclic motion. Additionally, rotational springs are used to enable the system to achieve resonance more easily. A simple system like this has already been shown to achieve flight, with a lift to drag ratio greater than 1 [8].

We have chosen a use a tail fin type design to passively stabilize the aerial vehicle which utilizes gravity, drag and lift to resist rotation away from an upright position. By avoiding additional actuators and sensors, the weight of the device can be minimized. To assist in the design process, we analyze the forces that destabilize the original FWMAV, looking primarily at the forces acting on the body of the vehicle by gravity and lift.

Force Analysis and Design:

The existing FWMAV design is composed of three components: the drive motor, elastic element and wing [8]. A helical spring is attached to the motor casing and motor cap which is connected to gear shaft. The wings are directly attached to the output shaft which allows for changing the wing flapping amplitude and mean flapping angle. The elastic structure of the wing, moment of inertia and drag enables a positive lift force in both strokes [9].

The angle of attack for each wing is constantly changing throughout the flapping phases. This change in attack angle is due to the flexible joint attaching the wing to the motor and produces different magnitudes of lift and thrust at different times of the wing stroke. To simplify our calculations, these forces are treated as averages over time.

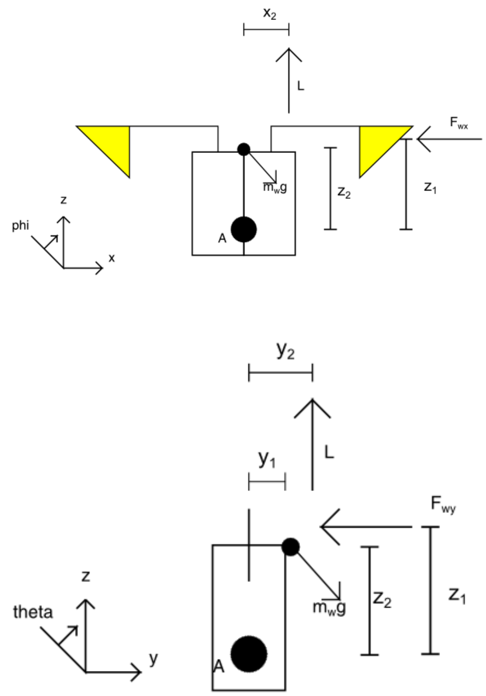

Figure 1 – Forces acting on the body of the FWMAV that cause instability.

The primary cause of rotation of a FWMAV comes from unbalanced forces produced by the wings, the resulting forces of which are visible in figure 1. These forces may stem from imperfections in fabrication or unequal actuation. Assuming that both wings are beating with the same frequency, if a single wing is flapping harder than its pair, it will produce more lift on one side of the FWMAV, thus offsetting the lift force (L) from the center, as well as inducing a net thrust perpendicular to the body (F_{wx}). It is also possible for unbalanced forces to arise if the center line of each wing's stroke is not parallel, favoring one side the device over the other. This would again offset the lift force and induce a perpendicular thrust (F_{wy}), as the wings are spending more time on one side of the FWMAV than the other. This can also offset the average center of mass of the wings (m_w).

The moments about the center of mass of the FWMAV motors (M_A) can be summed:

$$\begin{aligned}\sum M_{Ax} &= I_x\alpha_x \\ &= Ly_2 + F_{wy}z_1 \\ &\quad - m_w g\,(y_1 cos\theta + z_2 sin\theta)\end{aligned} \tag{1}$$

$$\begin{aligned}\sum M_{Ay} &= I_y\alpha_y \\ &= Lx_2 + F_{wx}z_1 - m_w g\,(z_2 sin\phi)\end{aligned} \tag{2}$$

Here, I and α are the moment of inertia and angular acceleration, with the subscript used to denote the axis about which they are related, and g is the acceleration due to gravity. The angles θ and φ are the relative tilt of the FWMAV from the upright position within the y and x planes respectively. The numerated x, y, and z values are the distances along the corresponding axis to the forces that create a moment about the center of mass of the motors (A). The center of mass of the motors is used as the motors comprise the overwhelming majority of the mass of the system. Assuming that the wings are well aligned, y_1 should be relatively small when compared to all other distances.

It can be seen from these equations that, in both planes, the lift and perpendicular forces cause rotation such that the tilt angles decrease (counter clockwise in figure 1), which will reduce the moments resisting the rotation if the angle is positive, or add to the rotational forces if the angle is negative.

After an initial analysis of the body forces on the FWMAV, design modifications were suggested to lower the center of gravity and add drag and lift forces encountered by the robot while tilting. The chosen passive stabilization system is that of a tail fin suspended below the FWMAV, as seen in figure 2. This fin adds a mass, drag and lift force that resists rotation from an upright orientation and alters the moment summation such that

$$\sum M_{Ax} = I_x \alpha_x = L y_2 + F_{wy} z_1 - m_w g\,(y_1 cos\theta + z_2 sin\theta) - D_y z_3 + m_f g (z_4 sin\theta) \quad (3)$$

$$\sum M_{Ay} = I_y \alpha_y = L x_2 + F_{wx} z_1 - m_w g\,(z_2 sin\phi) - D_x z_3 + m_f g (z_4 sin\phi) \quad (4)$$

With *D* being the drag and lift forces acting at the tail fin and m_f being the mass of the fin. As the robot tilts, the mass of the fin will apply a moment to restore the FWMAV to an upright position. The drag will resist fast rotations of the robot as it scales with the relative lateral speed of the air around (v_{lat}) the tail as drag is equal to $\frac{1}{2}\rho v_{lat}^2 C_D A_{cs}$, with ρ being the density of the fluid, C_D is the drag coefficient, and A_{cs} is the cross-sectional area of the fin.

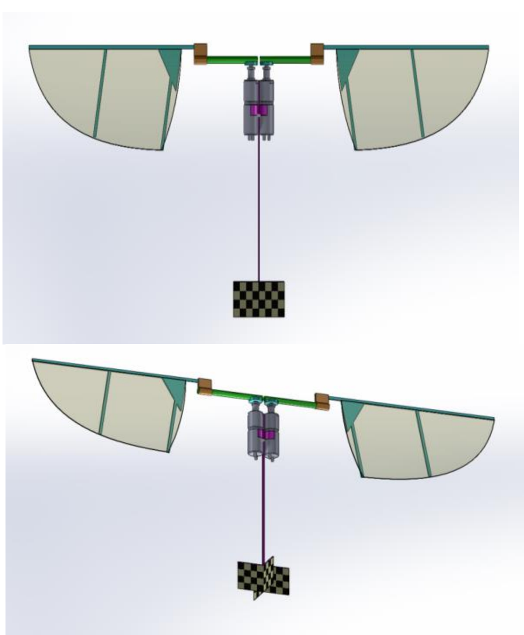

Figure 2 – CAD model of FWMAV with proposed tail fin stabilization device.

Lift may be generated by the tail fin while moving vertically (*z* direction) and rotating because the relative velocity of the air to the fin may have a positive angle of attack. The resulting force is $\frac{1}{2}\rho v_{tr}^2 C_l A_p$, *v* being the true velocity of the tail, C_l is the coefficient of lift, and A_p planform area of the fins. As these forces are highly dependent on the velocity of our FWMAV, these values are hard to predict without extensive simulation. It is important to note that both forces depend on the area of the fins. An updated free body diagram with the fin can be seen in figure 3.

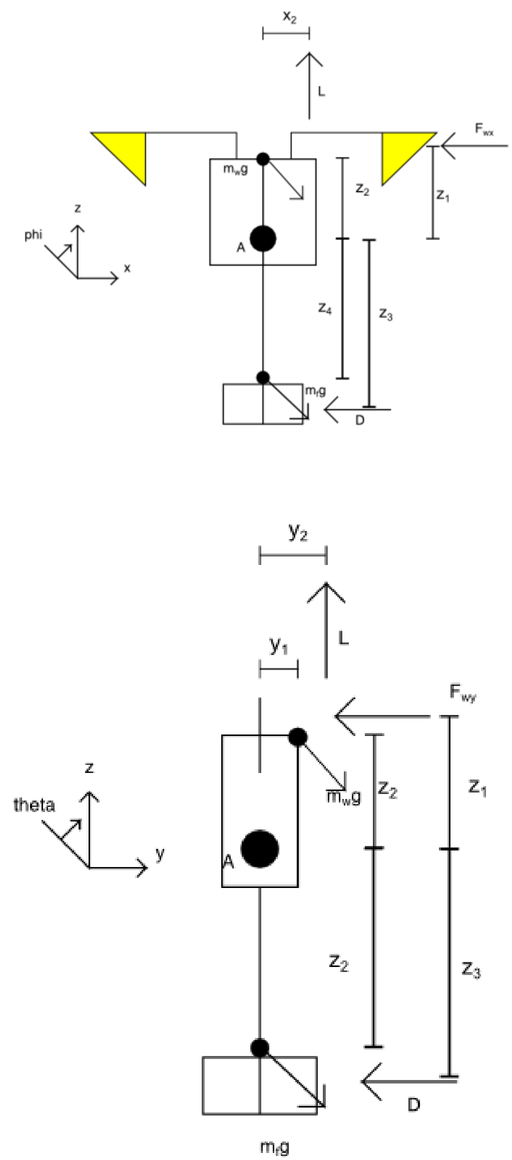

Figure 3 – Force acting on the body of the FWMAV with the fin included.

While it is possible to use a complex control system, sensors and a feedback loop to regulate the force output of each wing, this is outside of the scope of this project. The theoretical implication of its future incorporation is important in that it displays the advantages of have separately actuated wings. By precisely controlling the motors you can control the stroke angles and thereby control the attack angle of the wing. Asymmetry such as the ones described early can be purposefully induced to direct the FWMAV. Achieving lift off, hover, and movement in any given direction, our machine would be able to move in three dimensions.

Materials and Fabrication:

Lightweight materials are essentials to the fabrication of micro air vehicles. The purpose of these light materials is to reduce the weight of the entire robot, so that it is able to achieve lift off. The robot's ability to achieve this is by having a high power-to-weight ratio for it to be able to generate enough lift to attain take off. The main materials used are carbon fiber, found as rods and sheets, and thin Kapton® polymide film, both of which are extremely light weight for the strength they provide. Small laser cut acrylic parts are also used, as well as metal wire helical springs.

Prepreg carbon sheets are laser cut into tailored strips and bonded onto the Kapton® film to create a composite sandwich structure wings. The veins on the wings are necessary for reinforcement and to help it maintain its shape while flapping. Flexures made to allow the wings to rotate while flapping are made using a similar technique. The tail fin is made by simply bonding Kapton® film to carbon fiber rods.

The motors used are GM15A model micro motors produced by Solarbotics. The helical springs are found around the shaft of the motors, bonded to the motor casing and to the acrylic caps on the end of the shafts. The springs then induce a rotational stiffness that allows for resonance in the wing motion.

Completed FWMAV:

Design modifications included the addition of sail fins connected to robot at a distance of 90mm from the base of the motors. The fins act as dampers producing a restoring force during rotation. We chose to maximize the extension of the fins because, without extensive simulation of the fluid flow on the fins, we have little intuition as to the forces being produced on the sails. Mass is relatively fixed as we cannot have a weight larger than the lift being generated, so we opted to extend the fins out as far as possible while still maintaining a functional sail size, which we chose to be 25.4 mm by 25.4 mm. The fabricated design can be seen in figure 4.

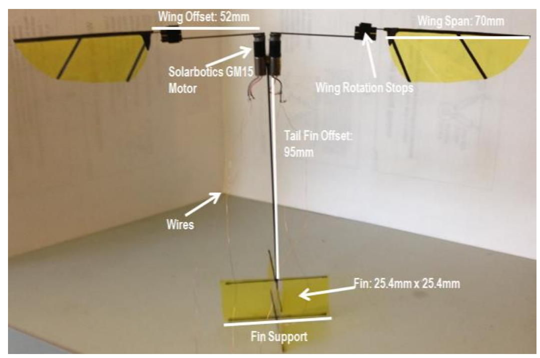

Figure 4 – Fabricated FWMAV with tail fin stabilization device.

Results:

The FWMAV developed has a total weight of 3.3 g and can create a max average 32 mN of vertical lift. This gives the robot a lift to weight ratio of approximately 1, but as our tests show that the FWMAV can lift off, this ratio is shown to be greater than 1. The mass of the FWMAV is composed mostly of the mass of the motors, of which each motor is 1.21 g.

The resonance frequency of the wings was found to be 10 Hz through experimentation. All tests are performed with the wings actuated at this frequency to maximize lift. Further experimentation lead was performed to find the lift generated by each wing as a function of the peak-to-peak voltage, one of these tests being shown in figure 5a. The maximum lift was found at a voltage of 14 V, the largest voltage applied, with the lifts being 14 mN and 17 mN for each wing. A list of all of the major FWMAV performance metrics can be seen in table 1.

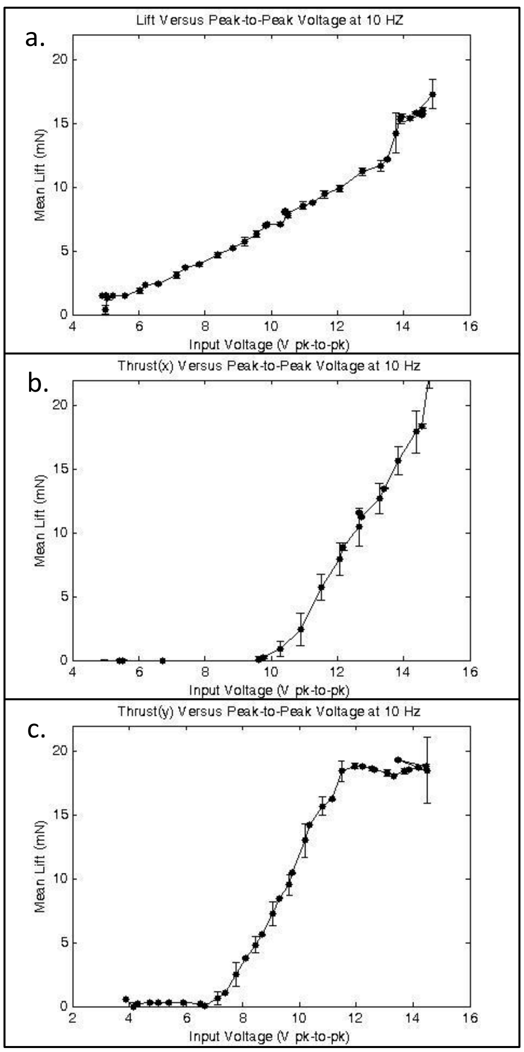

Figure 5 – Force as a function of peak-to-peak voltage at 10 Hz for a single wing for vertical lift (a), x directional thrust (b), y directional thrust (c).

Flight tests of the device have found a max flight time of 0.375 seconds. The flight time is counted from takeoff to when the FWMAV becomes unstable in the air and begins falling. Figure 6 shows pictures from a flight test at various time s, in which the destabilization of the FWMAV can be seen. Control tests of the same robot without the stabilizing tail fins resulted in a max flight time of 0.188 seconds, so the stabilizing sails effectively doubled the flight time.

Additional tests were performed on one of the wings to measure the forces generated in the lateral directions (*x* and *y* directions as according to figures 1 and 3). These tests found the force produced at 10 Hz and 14 V (peak-to-peak) is 18 mN in both directions. The test results can be seen in figures 5b and 5c. The robot and measuring system was seen to vibrate quite vigorously, so these measurements may be inaccurate. If these values are correct, it should be noted that they are larger than the vertical lift forces being generated by a single wing.

Table 1 - Robot Metrics

Metric	Value
Total Mass	3.3 g
Wing Mass	0.27 g
Motor Mass	1.21 g
Tail Mass	0.34 g
Max Wing Lift	14-17 mN (~32 mN total)
Max Wing Thrust (x)	18-20 mN
Max Wing Thrust (y)	18-19 mN
Lift to Weight Ratio	Slightly >1
Spring Stiffness	2.8e3 mN.mm/rad
Max Lift Frequency	10 Hz
Peak-to-Peak Voltage	14 V

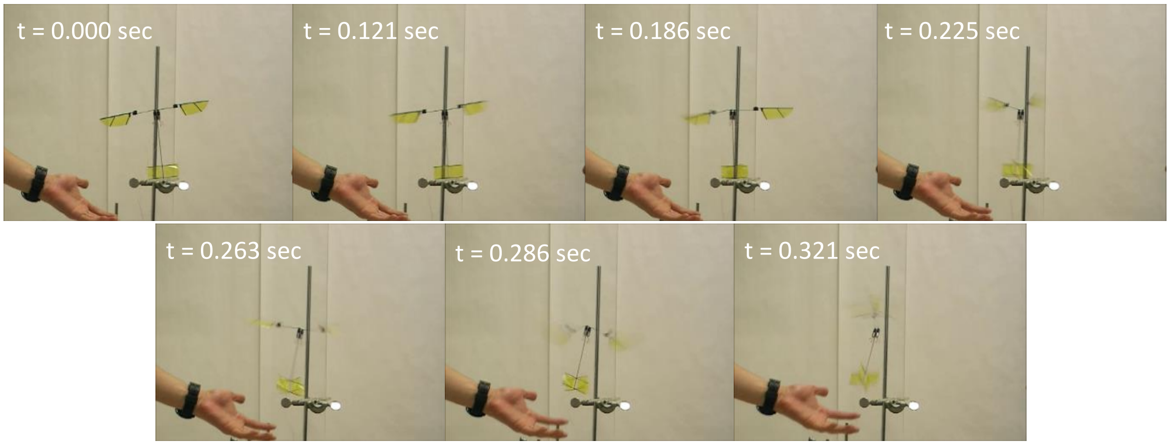

Figure 6 – Flight of the FWMAV with the stabilizing tail fin at various times during a test.

Discussion

Our stabilizing tail fin was found to increase the flight time of the FWMAV by almost twice the value of the control test, but this time is still quite limited, being less than a second. A variety of different features of the robot may potentially be contributing to this problem.

As previously mentioned, during some of our tests, the FWMAV was found to vibrate quite forcefully. These vibrations may be able to destabilize the robot in flight, as it may cause it to orient itself into undesirable positions. Additionally, the large mass of the motor dominates the system, so the use of mass as a form of stabilization is somewhat limited as the amount of mass that can be added is minimal.

The long length of the wing span, particularly from the wing offset, may be causing large torques on the system with each flap. The wing tips are moving long distance at a great speed, and so there will be large instantaneous drag forces. This can cause the robot to rotate or tilt while in flight. This can possibly be mitigated through changes in the wing size and shape, most likely using smaller wing offsets but larger wings (to maintain high lift), and a shorter total wing span.

It may also be necessary to add sails to the top of the FWMAV in addition to the bottom tail fins [9-11]. This is because it can move the pivot point, the center of drag forces caused by sails, above the center of gravity of the robot, which causes a far more stable system [9-11]. Employing this will require completely redesigning the current tail fin the so that a lift ratio above 1 can be maintained.

Conclusion and Future Work:

The design modifications increase the duration of flight but it is still not a stable system. One possible reason for instability is the pivot point (center of drag forces caused by sails) being lower than the center of gravity of robot which makes the entire system act as an inverted pendulum. [9]

Future work should focus on creating a new robot system with a pair of sail fins on top of the robot that raise the pivot point above the center of gravity and also try out various fin shapes and sizes to determine the pair that gives maximum stability. Additionally, the wing and wing offset sizes and shapes should be further examined to reduce any possible torques.

References:

[1] Karpelson, M.; Whitney, J.P.; Gu-Yeon Wei; Wood, R.J.; , "Energetics of flapping-wing robotic insects: towards autonomous hovering flight," Intelligent

Robots and Systems (IROS), 2010 IEEE/RSJ International Conference on , vol., no., pp.1630-1637, 18-22 Oct. 2010

[2] Baek, S.S.; Ma, K.Y.; Fearing, R.S.; , "Efficient resonant drive of flapping-wing robots," Intelligent Robots and Systems, 2009. IROS 2009. IEEE/RSJ International Conference on, vol., no., pp.2854-2860, 10-15 Oct. 2009

[3] Karpelson, M.; Whitney, J.P.; Gu-Yeon Wei; Wood, R.J.; , "Design and fabrication of ultralight high-voltage power circuits for flapping-wing robotic insects," Applied Power Electronics Conference and Exposition (APEC), 2011 Twenty-Sixth Annual IEEE , vol., no., pp.2070-2077, 6-11 March 2011

[4] Bronson, J.R.; Pulskamp, J.S.; Polcawich, R.G.; Kroninger, C.M.; Wetzel, E.D.; , "PZT MEMS Actuated Flapping Wings for Insect-Inspired Robotics," Micro Electro Mechanical Systems, 2009. MEMS 2009. IEEE 22nd International Conference on , vol., no., pp.1047-1050, 25-29 Jan. 2009

[5] Arabagi, V.; Hines, L.; Sitti,M.; , "Design and manufacturing of a controllable miniature flapping wing robotic platform." *The International Journal of Robotics Research 31*, no. 6: 785-800.; 2012

[6] Tanaka, H.; Wood, R.J.; , "Fabrication of corrugated artificial insect wings using laser micromachined molds." *Journal of Micromechanics and Microengineering* 20(7): 075008.; 2010

[7] Dawson, D.; "Repeatable Manufacture of Wings for Flapping Wing Micro Air Vehicles Using Microelectromechanical System (MEMS) Fabrication Techniques"; *Air Force Inst of Tech Wright – Patterson AFB OH Dept of Aeronautics and Astronautics* (No. AFIT/GAE/ENY/11-M06).; 2011

[8] Hines, L; Campolo, D; and Sitti, M; "Liftoff of a Motor-driven, Flapping Wing Micro Aerial Vehicle Capable of Resonance,"unpublished

[9] van Breugel, F; Teoh, Z E; and Lipson, H; "A Passively Stable Hovering Flapping Micro-Air Vehicle" in *Flying Insects and Robot, Floreano, D.; Zufferey, J.-C.; Srinivasan, M.V.; Ellington, C. (Eds.)*. New York: Springer, 2010, pp. 171-184.

[10] van Breugel, F; Regan, W; and Lipson, H.; "From Insects to Machines" in *IEEE Robotics and Automation Magazine*. Dec. 2008, pp. 68-74.

[11] Richter, C. and Lipson, H.; "Untethered Hovering Flapping Flight of a 3D-Printed Mechanical Insect"; Proc. of the Alife XII Conference, Odense, 2010, pp. 797-803.